High-resolution Electron Energy Loss Spectroscopy Study of O-Cu(410)

ARTICLE *in* THE JOURNAL OF PHYSICAL CHEMISTRY B · FEBRUARY 2007

Impact Factor: 3.3 · DOI: 10.1021/jp0667083 · Source: PubMed

High-resolution Electron Energy Loss Spectroscopy Study of O-Cu(410)

Luca Vattuone,* Letizia Savio, and Andrea Gerbi

Dipartimento di Fisica, Università di Genova and CNISM Unità di Genova, Via Dodecaneso 33, 16146 Genova, Italy

Michio Okada

Department of Chemistry, Graduate School of Science, Osaka University, Machikaneyama-cho, Toyonaka, Osaka 560-0043 Japan and PRESTO, Japan Science and Technology Agency, 4-1-8 Honcho Kawaguchi, Saitama, Japan

Kousuke Moritani

Synchrotron Radiation Research Center, Japan Atomic Energy Agency 1-1-1 Kouto, Mikazuki, Sayo, Hyogo 679-5148, Japan

Mario Rocca

IMEM-CNR and Dipartimento di Fisica, Università di Genova, Via Dodecaneso 33, 16146 Genova, Italy

Received: October 12, 2006; In Final Form: December 12, 2006

We have investigated oxygen adsorption on Cu(410) by high-resolution electron energy loss spectroscopy, dosing O_2 with a supersonic molecular beam at different surface temperatures and for different angles of incidence and beam energies or by backfilling. In the investigated crystal temperature range ($127 < T < 570$ K), adsorption is always dissociative. Depending on T, impact energy, and angle of incidence, the oxygen atoms end up in different adsorption configurations, characterized by different vibrational signatures. In particular, at grazing incidence when only the step edge is exposed to O_2, the adatoms end up initially preferentially at the step edge. An ordered overlayer forms at half monolayer coverage when the adsorbate is mobile. Oxide patches develop eventually for large exposures performed by backfilling and at high crystal temperature.

Introduction

Adsorption of oxygen on Cu surfaces has been investigated extensively[1] in the attempt to clarify the mechanism underlying Cu_2O formation.[2,3] Cuprous oxide is an industrially important direct-gap semiconductor with a band gap of 2 eV, promising for application to photovoltaic cells. Most investigations concentrated therefore on the high coverage regime required to start oxide formation. The initial stages of oxygen adsorption received relatively less attention. Several detailed investigations were performed by backfilling but, to the best of our knowledge, molecular beam studies exploring the angle, energy, and temperature dependence of the sticking probability were limited to O_2 adsorption at Cu(110)[4,5] and Cu(100).[6−8] In this paper, we report on a supersonic molecular beam study on O_2/Cu-(410). While the initial sticking probability data will be presented elsewhere,[9] we concentrate here on the vibrational analysis, which exhibits several intriguing features.

The present study was stimulated by recent papers trying to assess the adsorption sites[10] and the vibrational properties[11] of atomic oxygen on Cu(410) and by our previous investigations of oxygen adsorption on the similar, but less reactive, Ag-(410)[12,13] surface. For O/Ag(410), adsorption occurs both molecularly and dissociatively; access to the molecular state (stable below 150 K) is activated, while the direct nonactivated dissociative channel is connected to the steps. For the more reactive O_2/Cu(410) system, the interaction is direct and dissociative at all investigated temperatures ($127\ \text{K} < T < 570$ K) and for all dosing conditions. The adsorption sites reached by the O adatoms depend, however, on impact energy and angle of incidence of the gas-phase molecules and on crystal temperature.

Experimental Section

The experiments were performed in an ultrahigh vacuum chamber (UHV, base pressure in the low 10^{-10} mbar range) equipped with a self-built high-resolution electron energy loss spectrometer (HREELS), a low-energy electron diffractometer (LEED), a cylindrical mirror analyzer for Auger spectroscopy, and an ion gun for in situ cleaning and preparation of the sample.[14] A supersonic molecular beam is coupled to the chamber allowing dosage of O_2 at well-defined impact energy, E_i, and angle of incidence with respect to the surface normal, θ.

The sample is a 10 mm diameter disk, cut within 0.1° off the (410) direction. It is mounted onto a tantalum sample holder and can be heated by electron bombardment and cooled by fluxing liquid nitrogen through a cryostat. It was cleaned by cycles of 1.5 keV sputtering with Ne ions followed by annealing for 3 min to 900 K until clean. Auger and HREEL spectra and

* To whom correspondence should be addressed. E-mail: vattuone@fisica.unige.it.

10.1021/jp0667083 CCC: $37.00
Published on Web 01/31/2007

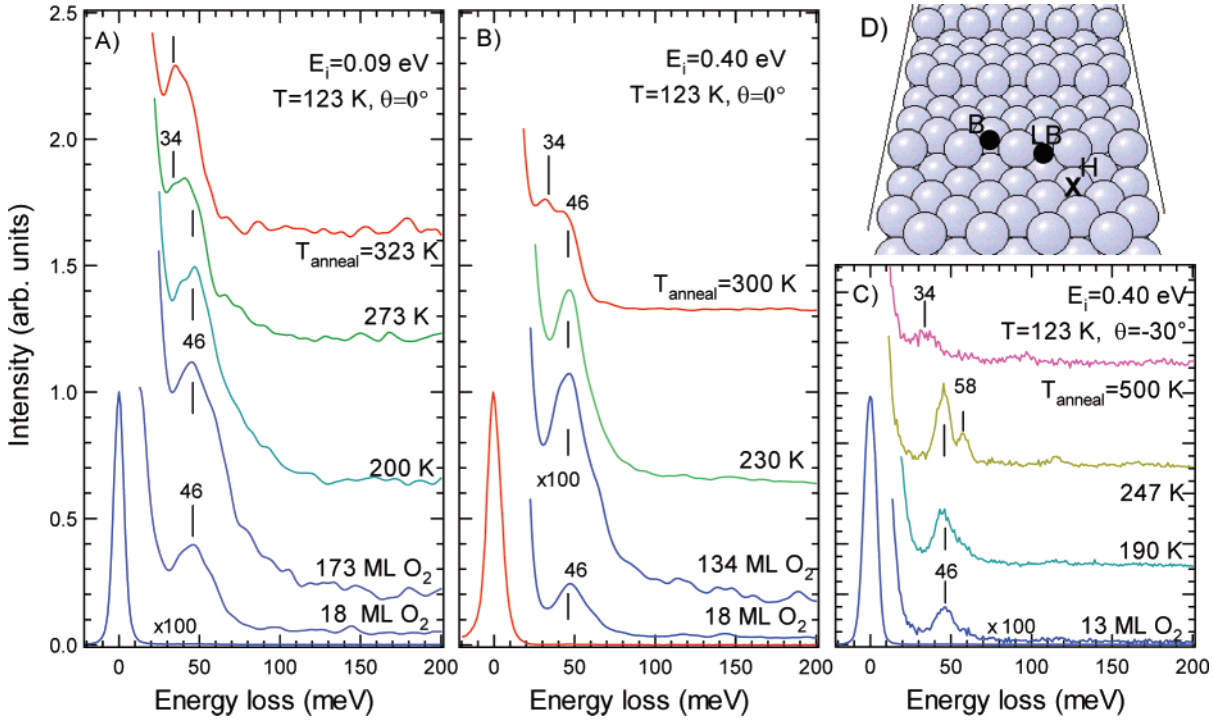

Figure 1. HREEL spectra recorded after dosing O_2 at $T = 123$ K and eventually flashing the Cu(410) crystal to different temperatures. Panels A and B show the spectra recorded after dosing normally to the (410) plane with $E_i = 0.09$ and 0.40 eV, respectively. Panel C corresponds to a dose performed with $E_i = 0.40$ eV and $\theta = -30°$, that is, off normal in the down step direction. Panel D shows the (410) surface geometry and the adsorption sites proposed by the theoretical model of ref 11. The loss at 58 meV is due most likely to traces of OH.[25] The scattering plane of both molecular and electron beams cuts the figure parallel to the long edge of the page.

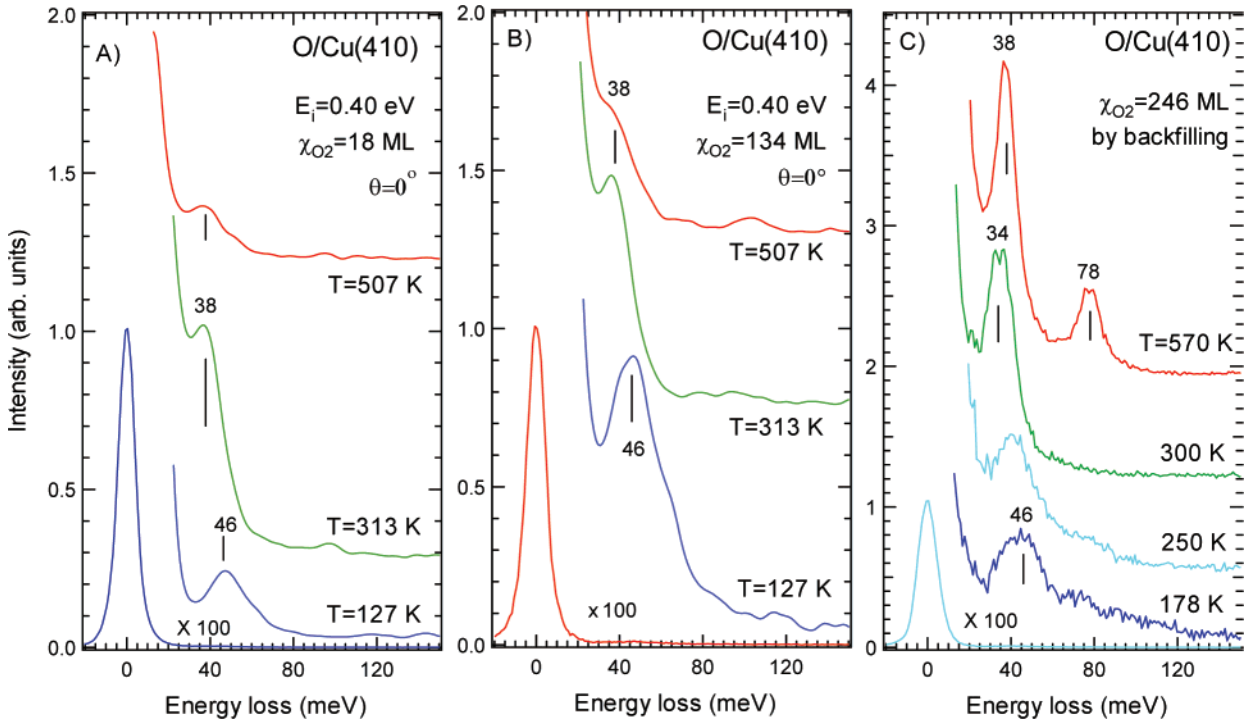

Figure 2. HREEL spectra recorded after exposing the Cu(410) surface at different temperatures to a supersonic O_2 beam seeded in He ($E_i = 0.40$ eV) and impinging at normal incidence for 420 s (panel A) and for 3120 s (panel B). Panel C shows spectra recorded after dosing 246 ML O_2 by backfilling.

a sharp LEED pattern were recorded. The surface geometry is shown in Figure 1D and consists of 3-atom-row wide (100) terraces alternated to monoatomic steps running in the <001> direction. A scanning tunneling microscopy (STM) investigation[15] showed fuzzy steps at RT, indicating that step roughening occurs below this temperature and that the open step edges are stabilized by oxygen.

O_2 was dosed either by backfilling the chamber or via the supersonic molecular beam. The beam translational energy, E_i, was varied in the range 0.09−1.4 eV by using either pure O_2 or O_2 seeded in He (4% concentration) and/or by heating the ceramic nozzle.

Care has been taken for calibration of the beam flux since the pumping system of the supersonic molecular beam has been

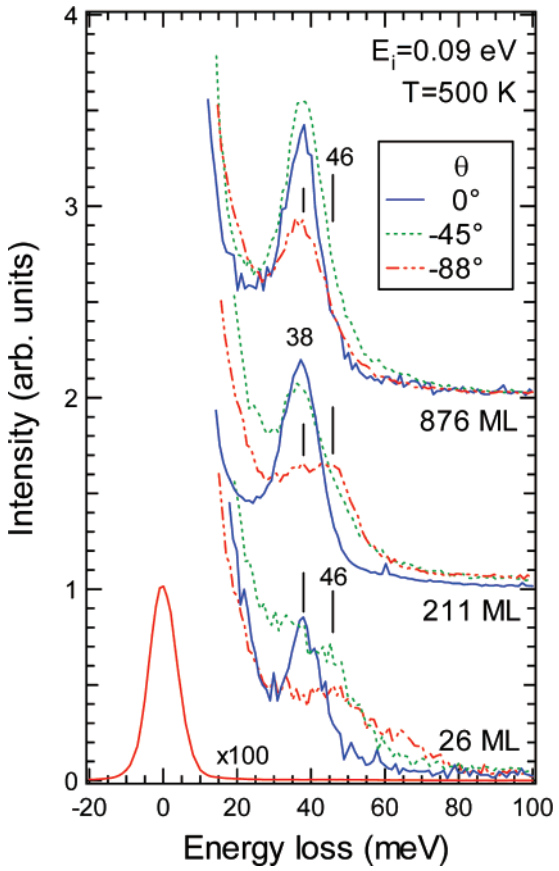

Figure 3. HREEL spectra recorded after dosing O_2 with $E_i = 0.09$ eV at different angles of incidence on Cu(410) at $T = 500$ K. Negative angles correspond to impingement conditions grazing to the step rise, which is shadowed for $\theta < -59°$. The exposure refers to the normal incidence experiments; therefore, for $\theta = -45°$ and $-88°$, it must be corrected by a cos θ factor (i.e., it is smaller especially for grazing incidence).

changed in the time between the first experimental runs and the latest ones. The flux has been calibrated with CO/Pd(100) experiments for which an inflection point is present in the sticking vs coverage curve at 0.3 ML; this point is taken as a reference[16,17] for calibration of the CO flux. The value for the O_2 flux Φ was then obtained from the CO flux after correcting for the ionization efficiency of the two gases. The seeded oxygen beam flux was obtained from that of the pure O_2 beam by comparing the increase in the quadrupole mass signal at mass 32 observed in the two cases when the beam enters into the main chamber. To compare the flux for different experimental runs, we used as a reference the pressure at the entrance of the rotary pump (which was the *same* for *all* the experiments reported here) backing the turbomolecular pump in the I stage (which was changed between the experiments of Figures 1 and 2 and those of Figure 3). This procedure yields $\Phi \approx 0.043$ ML-(O_2)/s for the pure and seeded beams of the experiments of Figures 1 and 2 and $\Phi = 0.11$ ML(O_2)/s for the pure beam of Figure 3 (1 ML $= 1.58\ 10^{15}$ atoms/cm^2).

The beam was collimated to a spot diameter of 8 mm at the sample, thus ensuring its uniform exposure and an optimal focusing condition for HREELS. Most HREEL spectra were recorded in-specular, at a primary electron energy $E_e = 2.7$ eV and at an angle of incidence of the electron beam of 60°.

Annealing the O covered surface causes a decrease in the loss intensity of the Cu−O stretch (40 meV) by more than a factor of 4 already when heating to 500 K. Heating to 870 K leads to a HREELS clean surface. Since, in agreement with the literature,[5] we observe no recombinative desorption, the O adatoms must move to subsurface sites, where they are no longer detected by HREELS. They are however still able to influence surface reactivity. Indeed, they affect the initial sticking probability of O_2 which is then smaller and recovers its normal value only after sputtering and annealing.

Results

In Figure 1, we report experiments in which O_2 is dosed by the supersonic molecular beam on the Cu(410) surface at $T = 123$ K and the layer is eventually flashed to higher temperature. Panels A and B refer to large exposures to O_2 beams impinging at normal incidence and with $E_i = 0.09$ and 0.40 eV, respectively; in panel C, we show data recorded after exposing the surface to a shorter dose with $E_i = 0.40$ eV and $\theta = -30°$ (corresponding to an incidence of 16° on the (100) nanoterraces and of 61° on the (110) nanoterrace (called step rises in the following)).

The following is apparent:

(a) No loss is present in the range from 75 to 110 meV, characteristic of molecularly chemisorbed O_2 (as reported, e.g., for Cu(111)[18]). This indicates that total O_2 dissociation occurs.

(b) After O_2 exposure at $T = 123$ K, a broad peak forms at 46 meV, for all dosing conditions.

(c) When annealing, another loss grows at 34 meV, whose intensity depends on dosing conditions.

Further data are shown in Figure 2. They were recorded after dosing O_2 at different temperatures. Panel A corresponds to a moderate exposure and panel B to a long exposure to hyperthermal O_2 dosed by the supersonic beam at normal incidence and panel C to similar experiments performed dosing by backfilling.

We find the following:

(d) Around room temperature (RT), the oxygen adatoms end up in states different from the one reached at low temperature. They are characterized by a loss at 38 meV when dosing with the hyperthermal beam and at 34 meV when dosing by backfilling at 300 K.

(e) Formation of Cu_2O (loss at 78 meV[19−21]) occurs only by backfilling and for $T > 500$ K.

(f) No losses are observed for $T > 870$ K (spectrum not shown).

In Figure 3, we show the HREEL spectra recorded after dosing O_2 by beam at different θ, with low translational energy and with the crystal at $T = 500$ K. The dosing angle affects the population of the different states. Indeed, at grazing incidence, a significant fraction of the adatoms ends up in the site vibrating at 46 meV, at least at low coverage. Since in this condition both step rises and most of the terrace area are in shadow, the O adatoms can only see the upper step edge (the (110) nanofacet corresponding to the step rise is not illuminated by the molecular beam). The overlayer structure forms eventually at larger exposure. It grows, on the contrary, immediately when dosing at angles close to the surface normal. Also, in these conditions, no oxide formation is observed even upon prolonged exposure at high temperatures (compare the uppermost spectrum in Figure 3 with uppermost spectrum in Figure 2C).

The 38 meV peak is observed also when dosing O_2 by backfilling at 570 K leading to the formation of an ordered structure identified initially by Thompson and Fadley as a "modified c(2 × 2)"[22] and characterized, more recently, by Vlieg et al.[10] According to these papers, the latter corresponds to half monolayer coverage with half of the oxygen at the step edge and other half at the fourfold hollows at the terraces. Only one

dipole active energy loss is, however, observed while two are expected by the two nonequivalent sites occupied by O.

Discussion

Our general conclusion is that the O adatoms generated on Cu(410) end up in different configurations depending on dosing conditions.

To try an assignment, we remind the reader that different phases with different dipole active vibrational signatures were reported also for O/Cu(100).[23] Oxygen adatoms on the unreconstructed surface vibrate thereby at 43 meV while their frequency decreases to 36 meV on the missing row reconstructed substrate. On Cu(110), O vibrates at 47.5 meV at 0.25 ML and at 48.9 meV at 0.5 ML coverage.[24]

The low-temperature state of O/Cu(410) (46 meV peak) could be due thus to atoms at fourfold hollows as well as to Cu−O chains forming at the step edge (in analogy to the Cu−O chains forming on Cu(110)). The latter hypothesis is less probable since Cu−O chains at the step are expected to be stable with respect to temperature, while we observe a shift to lower frequency when heating the crystal above 270 K.

A recent five-parameters Morse potential model calculation performed by Wang and Tian[11] for the O/Cu(410) system predicts a vibrational energy of 48 meV for oxygen adsorption at the bridge site (B) at the step (see Figure 1D). A mode at 47 meV was found, on the other hand, after dosing O_2 on Cu(100) at 100 K and was ascribed to the Cu−O stretch of O adatoms at bridge sites.[25] Since we estimate a coverage close to 0.5 ML after the long exposures of the experiments in Figure 1, that is, a value exceeding the step site density, we conclude that the 46 meV loss on Cu(410) corresponds presumably to O at bridge sites both at the step edge (B) and at the terraces.

According to ref 11, the B sites are metastable since the highest adsorption energy of 5.43 eV corresponds to adsorption at the long bridge (LB) site below the step. The calculated frequency of O at the LB is 40.2 meV and is thus very close to the one predicted for adsorption at the fourfold hollow (39 meV).

Both sites are occupied for the ordered overlayer. The predicted frequencies differ therefore by much less than our experimental resolution, thus justifying the observation of one single sharp loss at 38 meV in spite of the two expected by the nonequivalent adsorbates.

The sites predicted by the five-parameters Morse potential model[11] are however close, but not identical, to those determined by density functional theory (DFT) and by X-ray diffraction (XRD).[10] Further theoretical investigations of the dynamics of the system would therefore be useful for a definitive assignment.

The loss at 34 meV was not predicted by theory[11] nor observed on Cu(100). The frequency of 36 meV observed for O adatoms on the missing row reconstructed Cu(100) surface is however close to such a value. We tentatively assign this loss to the adsorption of isolated O at the LB site when no ordered O overlayer has formed. This assignment is however not very satisfactory since the computed frequency at the LB site is 40 meV and should not depend strongly on the order of the overlayer, unless ordering implies a different relaxation of the substrate atoms as is the case for O/Ni(100).[26,27] Oxygen adatoms compact into islands only if the temperature is high enough to allow for a sufficiently large mobility.

We notice that the spectroscopic signature (loss at 38 meV) of the ordered overlayer never dominates when O_2 is dosed at low temperature. Dosing O_2 at higher temperature seems thus necessary to obtain the ordered structure in spite of the fact that, at the highest beam flux, we estimate a coverage of 0.5−0.6 ML of atoms after an exposure of some monolayers at $E_i = 0.40$ eV at normal incidence, independent of temperature. The formation of the ordered phase is thus kinetically hindered. A similar conclusion was also reached for oxide formation.[28]

Indeed, as evident by comparing the spectra recorded after dosing 246 ML of O_2 by backfilling (upper spectrum in Figure 2C) and nearly 880 ML of O_2 exposure with the pure beam at normal incidence (upper spectrum in Figure 3), oxide nucleation is started only in the former conditions, that is, for a larger O_2 flux.

Our data show, moreover, that in the dissociation process the translational energy of the beam is partially transferred to the generated O adatoms, since the final state they reach depends on impact energy. Indeed, the HREELS signature of the formation of an ordered layer (38 meV loss) is observed already at RT when dosing O_2 at hyperthermal energy (see Figure 2).

Finally, we notice that at thermal energy and for very grazing incidence conditions the 46 meV site is populated also at high temperature (see Figure 3) at least in the initial stages of the uptake process. This finding is coherent with the assignment of this mode to O at the B site, since this is the only one exposed. The fact that oxygen survives in this state for the time needed to record the HREEL spectrum (tens of minutes with the sample at RT) indicates that diffusion into other adsorption sites is prevented by a high enough energy barrier.

It is worth comparing the behavior of the present system with the less reactive O−Ag(410).[12,13] For the latter, dissociation at low temperature occurs at the step edge only while at terraces O_2 adsorbs in a peroxide state. The higher reactivity of Cu(410) allows for total direct dissociation already at 127 K. While this happens also for Cu(100) and Cu(110), the availability of step edge sites favors the formation of stable Cu−O chains without the need of rearranging the substrate atoms. This allows the 0.5 ML coverage threshold beyond which cuprous oxide formation can start to be reached more rapidly.[28] The latter process is moreover probably favored also by easier oxygen incorporation at the open steps.

Conclusions

Three vibrational frequencies, corresponding to adsorption at different sites, have been observed for O/Cu(410). Comparison with the predictions of a five-potential Morse model calculation on the same system[11] allows for assignment of the highest energy loss (at 46 meV) to O adatoms at bridge sites. Such sites can be selectively populated at the step edges when dosing O_2 at grazing incidence, since they are the only sites exposed. At low temperature, oxygen atoms can moreover also populate terrace sites (presumably bridge sites) showing a very similar frequency. Upon annealing, oxygen moves irreversibly to a site vibrating at 34 meV, most probably the LB site indicated as the most stable by theory.[11] The experimental frequency is lower than that predicted (40 meV) but close to the one observed for O for the similar site at the missing row reconstructed Cu(100) surface.[23] When dosing O_2 at high temperature, an ordered phase forms at 0.5 ML coverage, corresponding to the formation of Cu−O chains at the step edge and to the occupation of fourfold hollows at the terraces. The O−Cu stretch then moves to 38 meV, with the vibrations at the nonequivalent sites being unresolved, in accordance with the very close values predicted by theory.[11]

Acknowledgment. We acknowledge financial support from Compagnia S. Paolo and MIUR (PRIN 2003).

References and Notes

(1) Yata, M; Saitow, Y. U. *J. Chem. Phys.* **2002**, *116*, 3075.
(2) Yang, J. C.; Yeadon, M.; Kolasa, B.; Gibson, J. M. *Appl. Phys. Lett.* **1997**, *70*, 3522.
(3) Okada, M.; et al. *J. Chem. Phys.* **2003**, *119*, 6994.
(4) Pudney, P.; Bowker, M. *Chem. Phys. Lett.* **1990**, *171*, 373.
(5) Hodgson, A.; Lewin, A. K.; Nesbitt, A. *Surf. Sci.* **1993**, *293*, 211.
(6) Hall, J.; Saksager, O.; Chorkendorff, I. *Chem. Phys. Lett.* **1993**, *216*, 413.
(7) Saitow, Y. U.; Yata, M. *Phys. Rev. Lett.* **2002**, *88*, 256104.
(8) Junell, P.; Ahonen, M.; Hirsimaki, M.; Valden, M. *Surf. Rev. Lett.* **2004**, *11*, 457.
(9) Vattuone, L.; Savio, L.; Okada, M.; Kasai, T.; Moritani, K.; Teraoka, Y. Manuscript in preparation, 2006.
(10) Vlieg, E.; et al. *Surf. Sci.* **2002**, *516*, 16.
(11) Wang, Z. X.; Tian, F. H. *J. Phys. Chem. B* **2003**, *107*, 6153.
(12) Savio, L.; Vattuone, L.; Rocca, M. *Phys. Rev. Lett.* **2001**, *87*, 276101.
(13) Vattuone, L.; Savio, L.; Rocca, M. In The Chemical Physics of Solid Surfaces. *Surface Dynamics*; Woodruff, D. P., Ed.; Elsevier: Amsterdam, The Netherlands, 2003; Vol. 11, Chapter 8.
(14) Rocca, M.; Valbusa, U.; Gussoni, A.; Maloberti, G.; Racca, L. *Rev. Sci. Instrum.* **1990**, *62*, 2172.
(15) Knight, P. J.; Driver, S. M.; Woodruff, D. P. *Chem. Phys. Lett.* **1996**, *259*, 503.
(16) Behm, R. J.; Christmann, K.; Ertl, G.; Van Hove, M. A. *J. Chem. Phys.* **1980**, *73*, 2984.
(17) Gerbi, A.; Savio, L.; Vattuone, L.; Pirani, F.; Cappelletti, D.; Rocca, M. *Angew. Chem., Int. Ed.* **2006**, *45*, 6655.
(18) Sueyoshi, T.; Sasaki, T.; Iwasawa, Y. *Surf. Sci.* **1996**, *365*, 310.
(19) Dawson, P.; Hargrave, M.; Wilkinson, G. R. *J. Phys. Chem. Solids* **1973**, *34*, 2201.
(20) Dubois, L. H. *Surf. Sci.* **1982**, *119*, 399.
(21) Baddorf, A. P.; Wendelken, J. F. *Surf. Sci.* **1991**, *256*, 264.
(22) Thompson, K. A.; Fadley, C. S. *Surf. Sci.* **1984**, *146*, 281.
(23) Wuttig, M.; Franchy, R.; Ibach, H. *Surf. Sci.* **1989**, *213*, 103.
(24) Pantforder, A.; Stietz, F.; Goldmann, A.; Courths, R. *J. Phys. C* **1995**, *7*, 5281.
(25) Sueyoshi, T.; Sasaki, T.; Iwasawa, Y. *Appl. Surf. Sci.* **1997**, *121/122*, 562.
(26) Rocca, M.; Lehwald, S.; Ibach, H. *Surf. Sci.* **1985**, *163*, Ll738.
(27) Franchy, R.; Wuttig, M.; Ibach, H. *Surf. Sci.* **1989**, *215*, 65.
(28) Okada, M.; Vattuone, L.; Gerbi, A.; Savio, L.; Rocca, M.; Moritani, K.; Teraoka, Y. Submitted for publication, 2006.